Int. J. Pharm. Investigation, 2025; 15(2):471-481.
https://www.jpionline.org

Original Article

Neuroprotective and Anti-Apoptotic Activity of Anthranilamide Pyrazolo[1,5-a] Pyrimidine Derivative against Parkinson's Disease Model in Rotenone-Induced SH-SY5Y Cells

Suresh Yerramsetty[1,4], Lavanya Ayyagari[1], Venkata Krishna Kanth Makani[1,3], Jolly Janette Mendonza[1,3], Suchitra Maheswari Ajjarapu[1], Ahmed Kamal[2,5], Smita C. Pawar[4,*], Manika Pal Bhadra[1,*]

[1]Department of Applied Biology, CSIR-Indian Institute of Chemical Technology (IICT), Tarnaka, Hyderabad, Telangana, INDIA.
[2]Division of Medicinal Chemistry and Pharmacology, CSIR-Indian Institute of Chemical Technology, Uppal Road, Tarnaka, Hyderabad, Telangana, INDIA.
[3]Academy of Scientific and Innovative Research (AcSIR), CSIR-Human Resource Development Centre, (CSIR-HRDC) Campus, Ghaziabad, Uttar Pradesh, INDIA.
[4]Department of Genetics and Biotechnology, Osmania University, Hyderabad, Telangana, INDIA.
[5]Department of Pharmacy, Birla Institute of Technology and Science (BITS) Pilani, Hyderabad Campus, Medchal, Telangana, INDIA.

ABSTRACT

Parkinson's Disease (PD) is the second most prevalent form of neurodegenerative disorder distinguished by progressive and specific loss of dopaminergic neurons in the Substantia Nigra (SNPc) resulting in abnormal movement and bradykinesia including multiple behavioral complications. Despite having diverse therapeutic approaches, noticeable reversals of the pathophysiological and behavioral features are yet to be observed. Here we report one of the Anthranilamide Pyrazolo[1,5-a] pyrimidine (known CDK inhibitors) derivate, C2 that has shown a neuroprotective effect in PD models of SH-SY5Y cells (neuroblastoma origin). This is one of the first studies that show C2 can act as a potent CDK1 inhibitor and additionally decipher its neuroprotective activity in Parkinson's disease. C2 neutralizes the rotenone-induced overexpression of pro-apoptotic caspases including caspases 9 and 3 and Bax. C2 showed neuroprotective activity and regulates neuronal cell death via modulation of p38/JNK MAPK family protein expression that are often dysregulated upon rotenone treatment. Collectively, these results implicate the role of C2 as a potential neuroprotective compound to treat PD pathogenesis. **Aim:** To investigate the neuroprotective and anti-apoptotic effects of an anthranilamide pyrazolo[1,5-a] pyrimidine derivative(C2) in a Parkinson's Disease (PD) model using rotenone-induced SH-SY5Y cells. **Background:** Although there are several therapeutic approaches, such as levodopa and carbidopa, that alleviate the transient symptoms of Parkinsonism, an effective drug candidate capable of decelerating disease progression and preventing neuronal apoptotic death has yet to be identified. **Materials and Methods:** To address this, we have used the rotenone-induced SH-SY5Y PD model to evaluate the protective role of C2 through functional assays. **Results:** We observed that C2 treatment reduces ROS production and provides protection to SH-SY5Y cells against apoptosis. C2 pretreatment improved cell viability and reduced apoptosis in SH-SY5Y cells exposed to rotenone, demonstrating its protective effects. C2 neutralizes the rotenone-induced overexpression of pro-apoptotic caspases including caspases 9 and 3 and Bax. C2 showed neuroprotective activity and regulates neuronal cell death via modulation of p38/JNK MAPK family protein expression that are often dysregulated upon rotenone treatment. Docking analyses showed that C2 binds to the ATP binding pocket of CDK1 with spontaneity comparable to other inhibitors, as indicated by ΔG values. C2 also interacts with the molecular fork like other inhibitors, suggesting it may be a potent CDK1 inhibitor, similar to Roscovitine. **Conclusion:** Our present study highlights that C2 has neuroprotective effects in the SH-SY5Y rotenone-induced PD model. Computational docking analyses revealed that C2 binds to the ATP pocket of CDK1 similarly to known inhibitors like Roscovitine, that shows neuroprotective properties. C2 reduces pro-apoptotic caspases (caspases-9 and -3) and Bax levels. Further, C2 also regulates p38/JNK MAPK protein expression, which is often dysregulated by rotenone. Collectively, these results implicate the role of C2 as a potential neuroprotective compound to treat PD pathogenesis.

Keywords: PD (Parkinson's Disease), Pyrazolo[1,5-a] pyrimidine derivatives, Rotenone, Dopaminergic neuron, CDK1, Molecular docking.

Correspondence:
Dr. Manika Pal Bhadra
Department of Applied Biology, CSIR-Indian Institute of Chemical Technology, Uppal Road, Tarnaka, Hyderabad-500007, Telangana, INDIA.
Email: drmanikapalbhadraiict@gmail.com; manikapb@gmail.com

Prof. Smita C. Pawar
Department of Genetics and Biotechnology, Osmania University, Hyderabad-500007, Telangana, INDIA.
Email: dr.smitapawar@osmania.ac.in; smita.prof@gmail.com

Received: 30-08-2024;
Revised: 25-10-2024;
Accepted: 18-12-2024.

OPEN ACCESS

Manuscript TECHNOMEDIA

DOI: 10.5530/ijpi.20250079

Copyright Information :
Copyright Author (s) 2025 Distributed under Creative Commons CC-BY 4.0

Publishing Partner : Manuscript Technomedia. [www.mstechnomedia.com]

INTRODUCTION

Parkinson's Disease (PD) ranks second in prevalence among neurodegenerative disorders, after Alzheimer's disease which results in progressive and selective degeneration of Dopaminergic (DA) neurons in the substantia nigra pars compacta projected from the striatum (Chinta and Andersen, 2005). Age is one of the major risk factors as it is rarely in the age group below 50 years, but the disease incidence increases 5 to 10-fold among people above 60 years (Reeve *et al.*, 2014). In most populations, very prominent gender biases have been observed in the case of PD -affecting males twice more than females (Van Den Eeden *et al.*, 2003).

In the last two decades, a substantial focus has been put forward on mitochondrial dysfunction and PD pathogenesis, as the majority of the pronounced candidate genes are involved in mitochondrial homeostasis (Choong and Mochizuki, 2023). Rotenone is found in nature, a pesticide prepared from the root and stems of tropical plant Derris and *Lonchocarpus* species, which can freely penetrate through the cell and mitochondrial membrane. (Caboni *et al.*, 2004). It is a potent mitochondrial complex I inhibitor, which interferes with oxidative phosphorylation and ATP production, thereby leading to the generation of ROS (Reactive Oxygen Species). Rotenone-induced ROS causes damage to different mitochondrial components and eventually results in apoptosis (Srivastava and Panda, 2007). Systematic rotenone administration causes selective degeneration of dopaminergic neurons of SNPc in animal models and induces PD-like pathophysiological conditions- providing a reliable platform for screening therapeutic drugs and small molecules as well as fundamental research on PD (Betarbet *et al.*, 2000).

To evaluate and enable the screening of novel neuroprotective agents, it is pivotal to screen against a disease model that replicates the pathology of PD. SH-SY5Y cells efficiently serve this particular purpose i.e., exhibit properties of dopaminergic neurons, which are primarily targeted in PD. Also, major features of Parkinson's include expression of α-synuclein, mitochondrial dysfunction and related oxidative stress are recapitulated in SH-SY5Y cells (Xicoy *et al.*, 2017). Due to their inherent ability to mimic the phenotypical characteristics of neurons and humanized origin, they serve as a potential source for drug screening in the context of human biology. With reference to earlier studies the Pyrazolo [1,5-c]quinazolines family scaffold that are a part of heterocyclic pyrazole structures, have garnered considerable interest from medicinal and synthetic chemists owing to their notable biological properties link inhibitors of CK2 kinase as well as compounds that are significantly evident to be utilized as the binding agent to GABA receptor and GABA neurotransmitters are known to be demented during Parkinson's (Ramu *et al.*, 2020; Guerrini *et al.*, 2013; Alharbi *et al.*, 2024).

In connection with the role of compounds in neurodegenerative disorders, our study also focuses on molecules of the Pyrazolo family. Anthranilamide Pyrazolo[1,5-a] pyrimidine derivatives, a novel class of pyrazolo-pyrimidine derivates with a modulatory role on the P53/MYCN axis and Cyclin-Dependent Kinases (CDK) (Ramaiah *et al.*, 2013). These CDKs are serine/threonine kinases best characterized for their impact on cell cycle regulation, but they are involved in various cellular processes including cell proliferation, migration, differentiation, metabolism and immune responses. Growing evidence implicates Cyclin-Dependent Kinases (CDKs) in the pathogenesis of multiple neurodegenerative disorders (Smith *et al.*, 2003). Considering previous reports, we have characterized a variety of novel derivatives of Anthranilamide Pyrazolo[1,5-a] pyrimidine and screened them in rotenone-induced SH-SY5Y neuroblastoma cells for their effect in lowering intracellular ROS levels, mitochondrial dysfunction and apoptotic damage. Anthranilamide Pyrazolo[1,5-a] pyrimidine derivatives were synthesized (Figure 1A) as described previously by Kamal, A. *et al.*, 2012.

MATERIALS AND METHODS

Cell culture

The SH-SY5Y cell line was obtained from the American Type Culture Collection and maintained in Dulbecco's Modified Eagle's Medium (DMEM), supplemented with 2 mM Glutamax, 10% fetal bovine serum, 100 U/mL Penicillin and 100 mg/mL Streptomycin sulfate. The cell lines were maintained at 37°C in a humidified atmosphere containing 5% CO_2 in the incubator.

MTT Cell viability assay

Cell viability was assessed by MTT assay, which assays mitochondrial function based on the ability of viable cells to reduce MTT to insoluble formazan crystals by mitochondrial dehydrogenase activity. SH-SY5Y cells were seeded in a 96-well plate at a density of $1x10^4$ cells per well. After overnight incubation, cells were treated with compounds and incubated for 24 hr. The cell culture medium was then discarded and replaced with 10 mL MTT dye. Plates were incubated at 37°C for 2 hr. The resulting formazan crystals were solubilized in 100 mL extraction buffer. The Optical Density (OD) was read at 570 nm with a micro plate reader (Multi-mode Varioskan instrument, Thermo Scientific) (Kona and Kalivendi, 2024).

Western blot analysis

Cultured cells were lysed with RIPA buffer (Sigma) and total cell lysate was quantified by Bradford assay. Western blotting was carried out by using an equal amount of Protein (50 mg per lane) applied to a 12% SDS-polyacrylamide gel. After electrophoresis, the protein was transferred to a Polyvinylidine Difluoride (PVDF)

membrane. The membrane was blocked at room temperature for 2 hr in 1X TBS+0.1% Tween 20 (TBST) containing 5% blocking powder. The membrane was washed with TBST for 5 min and the primary antibody was added and incubated at 4ºC overnight. Membranes were washed with TBST three times for 15 min and the blots were visualized with chemiluminescence reagent (Sahoo *et al.*, 2024).

Fluorescence-based microscopic analysis of ROS by H2DCF-DA Assay

To detect the levels of intracellular ROS generated H2DCF-DA staining method was performed. SH-SY5Y cells were treated with 4 µM C2 for 4 hr, followed by 100 nM rotenone exposures for 24 hr and stained with 1 uL of 20 µM DC-F-DA and incubated at 37ºC for 30 min. Post incubation, cells were washed with 1X buffer solution and then analyzed with a fluorescent microscope.

(DC-F-DA Excitation/Emission 485 nm/ 535 nm).

Fluorescence-based microscopic analysis of apoptosis

To detect viable and nonviable cells Acridine Orange and Ethidium Bromide (AO/EB) double staining method was performed. SH-SY5Y cells were treated with 4 µM C2 for 4 hr, followed by 100 nM rotenone exposures for 24 hr after which 50 µL of AO/EB dye mixture (10 µL/mg AO and 10 µL/mg EB in distilled water) in 1:1 ratio was added to each well of 24-well plate containing $2.5x10^4$ cells/well. Immediately after the incubation period, the cells were observed under fluorescent microscope (Acridine orange Excitation/Emmision 475nm/535nm; Ethidium bromide Excitation/Emission 525 nm/660 nm).

Caspase-3 and Caspase-9 assay

Caspase-3 and caspase-9 activity was determined by using Pan Caspase Inhibitor Z-VAD-FMK (Catalog Number: FMK001) according to the manufacturer's protocol. SH-SY5Y cells ($2×10^5$ cells/mL) were incubated at 4 µM C2 for 4 hr, followed by 100 nM rotenone exposures for 24 hr. Followed by pretreated with a pan-caspase inhibitor, 100 µM z-VAD as a positive control that can inhibit both caspase-3 and caspase-9 activities and protect against cell death Cells were harvested and lysed with lysis buffer. The supernatant was collected and protein concentration was detected by using Bradford's reagent. Caspase-3 and Caspase-9 activity was determined by measuring changes in absorbance at 505 nm using the Multimode reader.

Sequence retrieval and Structure analysis of selected protein

The amino acid sequence of CDK1 protein was retrieved from the Uniprot database with accession number P06493 elucidated using the Protparam tool of the Expasy server. The factors such as physicochemical properties, molecular weight, Isoelectric point (pI), half-life, Instability Index (II), Extinction coefficient (EI), Grand Average Hydropathy (GRAVY) and site of origin were analyzed. The Secondary Structure properties were estimated using the RAMPAGE server to estimate configuration scores like the total number of helices, turns, coils and predicted solvent accessibility, with the range (0 to 9) i.e. (highly buried- exposed region) based on the residue exposed. Z score is measured to predict residues that combine template and profile-based prediction of residues higher than zero (denotes less stable condition).

Model Assessment and Validation of the Protein Structure

The quality of the CDK1 Protein (CDK1/cyclin B) was tested for stability and reliability of the model structure. PROCHECK suite estimates the stereochemical quality of the model in the most favorable zones by quantifying residues. This quantifies the geometry of each residue as compared to the overall structure geometry. ERRAT tool statistically checks the non-bonded interactions between different atom types as a measure of the quality factor of the protein model (Colovos and Yeates, 1993). VERIFY3D determines the compatibility of the 3D atomic model with its amino acid sequence. ProSA tool validates the minimized structure for folding energy in the native protein. Consequently, UCSF Chimera was subjected to energy minimization.

Ligands were retrieved from PubChem Library. Likewise, the Ligprep tool was used for the preparation of high-quality structures. Parameters such as the addition of hydrogens, 2D to 3D structures conversion, bond angles and bond length were corrected with lower energy, stereochemistry and ring conformation followed using minimization potential of OPLS 2005 force field was changed. However, ionization did not change and tautomers were not generated through retaining their chirality. Compounds with the lowest energy were chosen for further study.

Preparation of Protein molecule and Active site Prediction

The target sequence file was uploaded in the workspace of the UCSF Chimera server. All the polar, nonpolar hydrogen atoms were added and solvents were removed, nonstandard residues

Table 1: The residues that interact with C2 are highlighted in red.

Glu8	Ile10	Glu12	Val18	Lys20	Ala31	Lys33	Val64	Phe80	Glu81
Phe82	Leu83	Ser84	Met85	Asp86	Lys89	Gln132	Leu135	Ala145	

were fixed. Gasteiger charges were assigned and Protonation states of His, Gln and Asn were added using the AMBER force field.

Receptor grid generation and Molecular Docking

Prior to molecular docking, a receptor grid was generated based on scoring functions using UCSF Chimera. The gird exploits a component of DOCK-a type of force field scoring. Followed, scores were implied to Vander Waals and electrostatic components on each receptor site for at least once. Molecular Docking was performed orderly by estimating energy for binding of the protein. This approach exploits computational methods and evaluates specific poses with ligands flexibility. Once, the molecular docking has been completed, the view dock interface displayed the scores. The G score denotes the binding energy of the pose and was calculated as below:

G score=a*vdW+b*Coul+ Lipo+Hbond+
Buryp+RotB+Metal+Site

where vdW-Vander Waals energy, Coul-Columb energy, Lipo-lipophilic contact, H-bondhydrogen bonding, Metal-metal-binding, BuryP-penalty for buried polar groups, RotB-penalty for freezing rotatable bonds, site- polar interactions within the active site and a=0.065 while b=0.130 are of the coefficients of vdW and Coul.

Statistical Analysis

Statistical analysis was performed using GraphPad Prism version 9.0. Data are presented as mean±SD of three independent experiments in each group.

RESULTS

C2 acts as a CDK1 inhibitor, similar to Roscovitine

C2 is an anthranilamide-pyrazolo [1,5-a] pyrimidine conjugate which is a selective combination of Pyrazolo[1,5-a]pyrimidine derivative and an anthranilamide moiety both known for their unique functions (Figure 1A). Pyrazolo [1,5-a] pyrimidine derivatives have been stated as CDK inhibitors, involved in cell proliferation and anthranilamides are tumor suppressive. Another classical CDK inhibitor is roscovitine, which belongs to the family of purines and inhibits CDKs by antagonizing with ATP for the ATP-binding site of the target kinase by interfering with amino acids that shape the ATP-binding pocket of the CDK catalytic triad (McClue *et al.*, 2002). Roscovitine is a pan purine analog inhibitor, which reduces CDK1, CDK2, CDK5, CDK7and CDK9 activity, but is a poor inhibitor of CDK4, CDK6 and CDK8 (Cicenas *et al.*, 2015). In context of the similar studies, we investigated the role of compound C2 which belongs to an anthranilamide-pyrazolo [1,5-a]pyrimidine conjugate family as a CDK inhibitor. To check which CDK is impacted by C2 treatment, cell cycle analysis using Flow cytometry was analyzed from the previous study. Cell accumulation at the sub-G1 phase represents apoptosis and C2 additionally shows accumulation at the G2/M checkpoint (Figure 1B, 1C). This G2/M arrest indicates that the cells are prevented from entering the mitotic phase which gives C2 a potent anti-cancerous activity.

In particular, the activity of the Cyclin B-cdc2 (CDK1) complex is crucial in regulating the G2-M phase cell-cycle transition, therefore studying whether C2 can act as a CDK1 inhibitor is significant. Therefore CDK1 was docked against C2 and Roscovitine to visualize the binding of both compounds to the protein (Figure 1D, 1E). Docking was carried out using Swiss Dock and the docked structures were analyzed using UCSF Chimera (Pettersen *et al.*, 2004) (Pettersen *et al.*, 2004). The structure of CDK1 used was 6gu2.pdb. Before docking the ligand and additional chains were also removed. Hydrogens and charges were added using Dock prep of UCSF Chimera. The G score of the CDK1 inhibitors was found to be in the range of 7.096 for isopentenyladenine and 10.328 kcal mol^{-1} for purvalanol B, with a mean value of -8.955 kcal mol^{-1} and Delta G of C2 binding to CDK1 is -10.294742 kcal mol^{-1}. The delta G value is comparable to the known value of Roscovitine binding of -10.318 kcal mol^{-1} (Saraiva *et al.*, 2011). To check the nature of the active site, hydrophobicity of the surface of the protein and binding sites of roscovitine as well as C2 was checked. With colors ranging from the most hydrophilic residues (dodger blue) to 0.0 (white) and to the most hydrophobic residues (orange-red), the hydrophobicity surface illustrates the hydrophobic nature of amino acids. Surface binding analysis revealed that both Roscovitine and C2 bind to the identical active catalytic site which forms a hydrophobic cleft/pocket on the surface of the CDK1 protein. The main residues in the binding pocket/active site of CDK1 are shown in Table 1.

The interacting residues of C2 with the binding pocket were analyzed and were found to interact with the following residues as shown in Figure 1F. The GLU81 and LEU83 that form a molecular fork conserved in many of the CDKs are also present in CDK1 and were found to be interacting with C2. The spatial arrangement between the inhibitor and NH on LEU83 is 1.913A°. The spatial arrangement between inhibitor and C=O on LEU83 is 2.673 A°. The docking study shows that C2 binds to the catalytic region (ATP binding pocket) of CDK with a comparable spontaneity as that of other inhibitors, as seen by the delta G values and C2 also interacts with the molecular fork as seen in other inhibitors. These results indicate that C2 may act as a potent CDK1 inhibitor similar to roscovitine. Roscovitine is known to have neuroprotective effects[1,2] therefore in the current study we check whether C2 has neuroprotective effects in neurodegenerative Parkinsons disease.

C2 Protects cells from Rotenone-Induced Cell Death and imbalance in ROS generation

SH-SY5Y cells were cultured in 96-well plates with a cell density of 3×10^3 cells per well. To assess the therapeutic potential of C2 against rotenone toxicity, cells were cultured under various concentrations of C2 (0. 25, 0. 5, 1, 2 and 4 μM) for 4 hr followed by rotenone (100 nM) treatment for 24 hr. The results depicted that C2 at 4 μM concentration had protective effect against rotenone induced cytotoxicity. According to the dose-dependent response by MTT assay, the concentrations of C2 at 4 μM and rotenone at 100 nM were taken forward.

Intracellular ROS levels generated were determined by measuring the fluorescence generated by H2DCF-DA (2′, 7′-dichlorodihydrofluorescein diacetate). Non-fluorescent H2DCF-DA is a probe that enters the cells by passive diffusion and is then metabolized by intracellular esterases to form a DCFH carboxylate anion. The oxidation of the DCFH by the intracellular ROS agents such as superoxide, H2O2 and peroxynitrite leads to the formation of highly fluorescent 2',7'-Dichlorofluorescein (DCF) that measures the amount of intracellular ROS (Kalyanaraman *et al.*, 2012). Green fluorescence intensity was higher in the rotenone-treated cells suggesting the formation of high ROS levels. When C2 was pretreated to the rotenone-exposed cells, the green color intensity was reduced suggesting that the intracellular ROS formation was decreased (Figure 2A, 2B), thus suggesting that C2 reduces intracellular ROS level produced by Rotenone. Hence, the findings provide evidence for the proposition that C2 has a neuroprotective effect against ROS-mediated degenerative processes that occur in PD. To understand the role of C2 in protecting against apoptosis, AO/EB staining of SH-SY5Y cells with rotenone and C2-treated cells was done (Kasibhatla *et al.*, 2006). This technique distinguishes the living and the dead cells. Acridine orange enters both live and dead cells, fluorescence green when bound to DNA and fluorescence red when it binds to RNA. On the contrary, ethidium bromide binds particularly to dead cells and DNA where the membrane is damaged and emits red fluorescence. The control cells that were not treated with the compound did not exhibit any change in the morphology as observed from their brightness in the fluorescence. On the other hand, cells exposed to 100 nM rotenone were observed to have an orange luminescent apoptotic body. However, when cells were pretreated with C2, cell viability was enhanced and apoptotic cell death was reduced in comparison with only rotenone treated cells (Figure 2C, 2D).

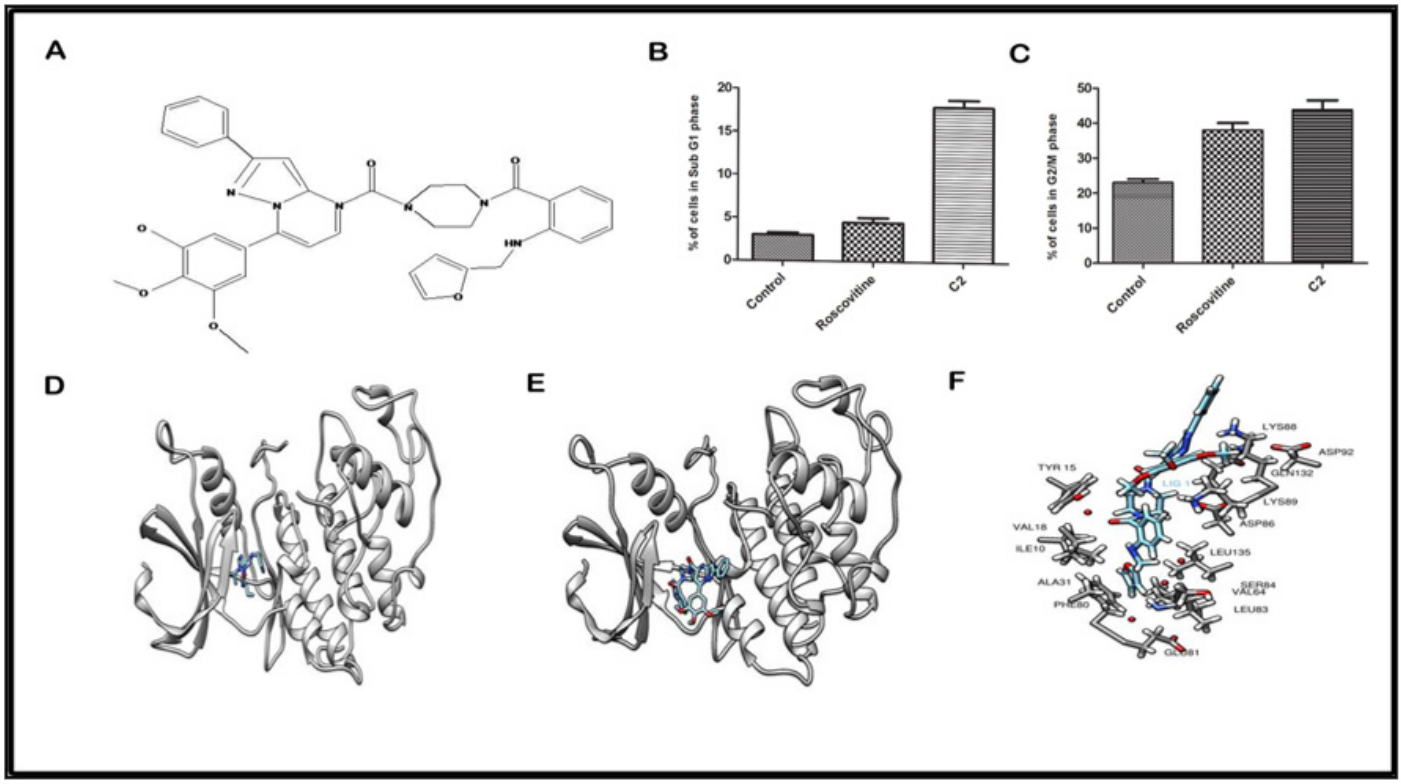

Figure 1: C2 treatment arrests the neuroblastoma cells at the G2/M phase of the cell cycle by binding to CDK1.

(A) Structure of C2:(4-(2-(furan-2-ylmethylamino) benzoyl) piperazin-1-yl)(2-phenyl-7-(3,4,5-trimethoxyphenyl)pyrazolo[1,5-a]pyrimidin-5-yl)methanone. **(B, C)** Flow cytometric analysis based graphical depiction of cell cycle phases at sub-G1 and G2/M upon C2 treatment in neuroblastoma cells. **(D, E)** Docked structure of roscovitine and C2 with CDK1, respectively. **(F)** The interacting residues of C2 with the binding pocket of the CDK1 protein.

C2 prevents changes induced by Rotenone in the expression levels of apoptotic and p38-JNK signaling proteins.

Next, to understand the mechanism of action by C2 on apoptosis induced by rotenone, we examined the role of C2 on the expression levels of both anti-apoptotic and pro-apoptotic proteins by western blot analysis. In comparison to control cells, rotenone-treated cells exhibited a significant reduction in the expression of Bcl-2 and Cyt-c in the mitochondria and an increase in the expression of Bax, caspases-3, 8 and 9. Treatment of rotenone significantly decreased the Cyt-c translocation into the cytosol. Prior treatment with C2 gradually recovered the imbalance in the expression of these proteins. In contrast, though the treatment of C2 on SH-SY5Y cells, showed no effects in the control condition when treated along with rotenone produced noticeable alterations in the expressions of apoptotic markers at the protein level including signaling pathway markers like p-P38, p-JNK and p-ERK (Figure 3A, 3B, 3C). In Rotenone treated condition Bax expression was elevated and Bcl-2 level was reduced indicating rotenone-induced mitochondria-mediated cell death. Interestingly, C2 treatment following rotenone induction was found to reverse the expression of Bcl2 and Bax significantly like untreated conditions- providing insights into the neuroprotective function of C2. Besides this, we have also observed increased expression of cytosolic Cytochrome-c upon rotenone treatment-which promotes the assembly of apoptosome (Chipuk and Green, 2008). One of the components of apoptosome *i.e.* Apaf-1 directly interacts with caspase-9 and activates caspase-9 through conformational change (Qin *et al.*, 1999). Activation of caspase-9 triggers executioner caspase-3 to

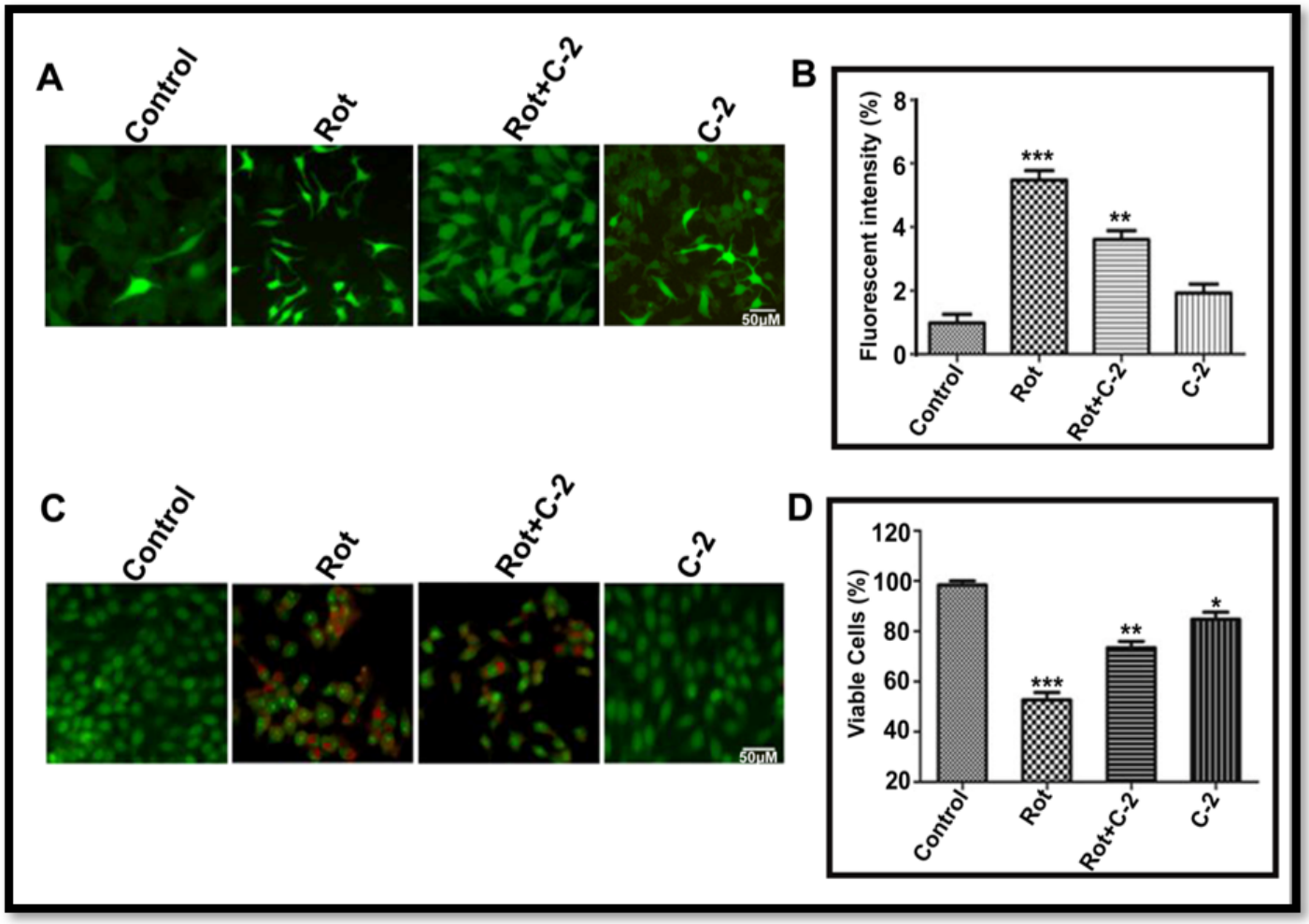

Figure 2: C2 induces a reduction in ROS production and protects SH-SY5Y cells against apoptosis.

(**A**) Fluorescent microscope pictures of SH-SY5Y cells showing loss of fluorescent intensity in C2 pretreated cells depicting a decrease in ROS production compared to rotenone-treated cells. (**B**) Histograms depicting comparative measurement of ROS production in cells upon C2 treatment. Treatment with 100 nM rotenone resulted in a significant increase in reactive oxygen species (ROS) levels compared to the untreated control cells. Conversely, pretreatment with C2 at 4 µM markedly decreased ROS levels in comparison to cells that were only exposed to rotenone. (**C**) Furthermore, the photomicrograph demonstrates the protective anti-apoptotic effect of C2 (4 µM) in the presence of 100 nM rotenone treatment. (**D**) Histograms depicting comparative measurement of apoptotic cells upon C2 pretreatment compared to untreated cells and rotenone-treated cells. The values are presented as the mean±Standard Deviation (SD) derived from three independent experiments conducted within each group. The scale bar indicates 50 µm.

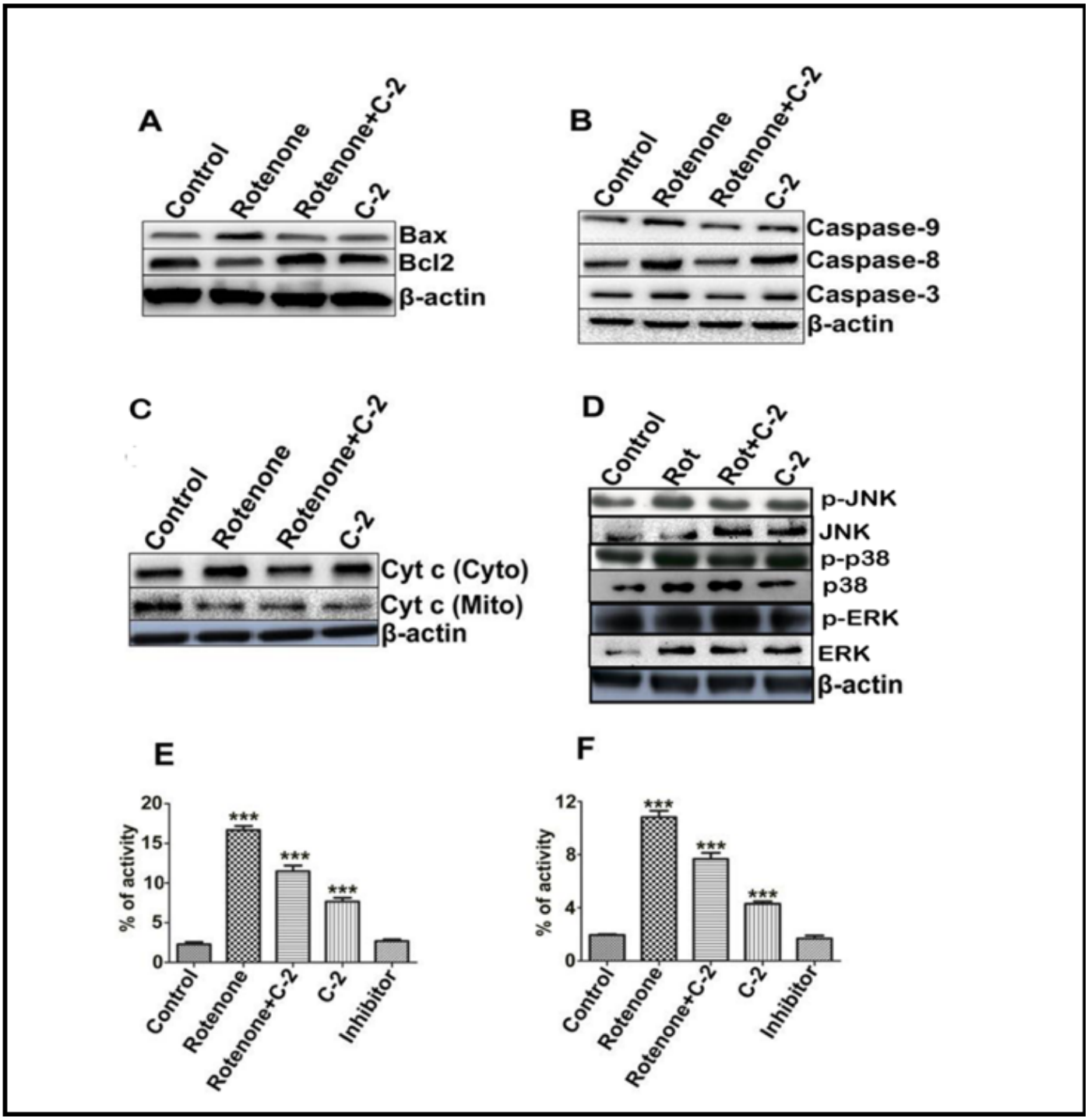

Figure 3: Western blot analysis showing the effect of C2 on the expressions of apoptotic and signaling markers.

(A,B and C) Western blotting analysis indicating increased expressions of Bax; caspase-3, caspase-8, caspase-9 and cytosolic Cyt-c and decreased expressions of Bcl-2 and cyt-c in mitochondria in rotenone treated group as compared to the control. Pretreatment with C2 restored the imbalance in the expression. (**D**) Rotenone treatment stimulates the expressions of p-JNK, p-P38 and p-ERK as compared to the control. Pretreatment with C2 decreases the expressions of p-JNK, p-P38 and p-ERK significantly. (**E, F**) Time-dependent increase of Caspase-3 and Caspase-9 activity after Rotenone exposure. Treatment of C2 and Z-VAD (pan-caspase inhibitor, positive control) significantly reduced Rotenone-induced caspase-3 and caspase-9 activation. In all the experiments β-actin has been used as a gel loading control.

carry out mitochondria-mediated apoptosis (Slee *et al.*, 1999). At the same time, Rotenone also upregulated the caspase-8 protein that is involved in extrinsic apoptotic pathways via attaching to death receptors (Kantari and Walczak, 2011). As with caspase-9 and caspase-3, C2 treatment decreased the up-regulation of caspase-8-further indicating that C2 is neuroprotective against both the mitochondria-mediated and an extrinsic apoptotic pathway. To know the process by which rotenone kills cells

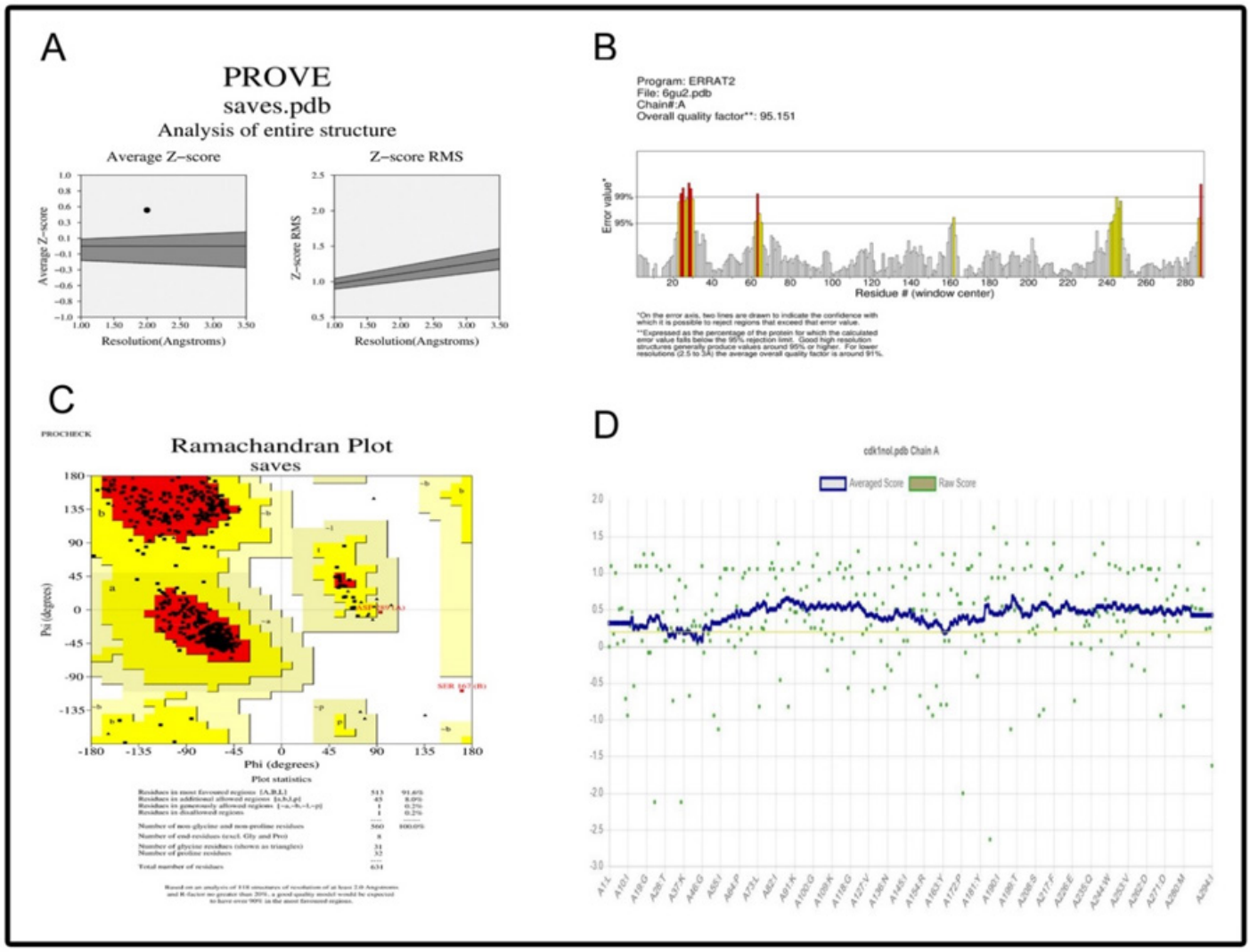

Figure 4: Structure validation scores using SAVES server 6.0 for CDK1.

(A) The protein measure deviations of both average Z score and RMS Z score from the standard atomic models as a quality measure of a protein crystal. **(B)** The CDK1 protein represents the statistics of highly refined structures as an average quality factor. **(C)** Ramachandran plot of CDK1 depicts the amino acids ((91.6%) in the most favored region. **(D)** The VERIFY3D tool presents the compatibility of the atomic model (3D) to its primary sequence.

and how C2 exerts the protective effect, the expression pattern of signaling proteins was done. The levels of p-P38, p-JNK and p-ERK were considerably higher in rotenone-treated cells in comparison with the control. After treatment with C2 prior to rotenone, there was a significant reduction of p-P38, p-JNK and p-ERK proteins. However, as compared with the treatment of C2 alone to control cells, there was a minimal alteration in the expression of p-JNK, p-P38 and p-ERK proteins (Figure 3D).

This study has revealed that Rotenone triggers apoptosis in neuronal stem cells via initiation of caspase cascade (Li *et al.*, 2005). To further explain if C2 reduces caspase-3 induced by rotenone and activates caspase-9 on rotenone induction, the cells were initially treated with 4 µM C2 for 4 hr and then treated with 100 nM rotenone for 24 hr. 100 µM z-VAD, a pan-caspase inhibitor was used as a positive control for the experiment to inhibit both caspase-3 and 9. In line with the previous studies, the present study also observed that 100 nM rotenone augmented both the caspase-3 and 9 activities, which were substantially reduced in C2 pretreated cells (Figure 3E, 3F).

Model assessment and structural analysis of CDK1 protein structure

To study the structural aspects of CDK1, the sequence was retrieved from 6GU2 (Uniprot ID: P06493). Parameters such as physiochemical properties, molecular weight, theoretical PI (isoelectric point), half-life, Instability Index (II), Aliphatic Index (AI), Extinction Coefficient (EI), Grand Average hydropathy (GRAVY) and site of origin were measured using Protparam tool in Table 2. Prediction of the secondary structure was performed using the PROCHECK server as the most favored residues fall at 91.6% (including the total no. of helices, turns and coils) depicted in Figure 4C. The stereochemical quality of the PROCHECK server shows the detailed deviations and properties

Table 2: The Primary sequence analysis using the ProtoParam tool of CDK1 protein.

Parameters	CDK1
Molecular weight (kD)	34.95.45
pI	8.38
Aliphatic Index	97.78
Instability Index	39.26(stable)
GRAVY	-0.281
Atoms	7772
Asp+Glu	37
Arg+Lys	39

at the residue level that contribute to the reliability and stability of the protein structure of CDK1. The significance was that it assesses the overall quality of the structure when compared with refined structures of the same resolution. Overall, this confine a protein model CDK1 as stable and was processed for further study. ERRAT tool has measured 95.15% on the statistical data on non-bonded interactions among several types of atoms contributing to the overall quality factor of the protein in Figure 4B. Similarly, regarding the affinity of the atomic model (3D) the tool VERIFY_3D has shown 93.82% of the residues averages a 3D-1D score of >=0.2 while the PROVE tool shows the buried outlier protein atoms are 2.6% (Figure 4A, 4D). All the above analysis was carried out using Structural Analysis and Verification Server.

DISCUSSION

In the current study, we show that C2 can act as a CDK1 inhibitor similar to Roscovitine which shows a neuroprotective effect via CDK1 inhibition. This is one of the first studies that shows C2 can act as a potent CDK1 inhibitor which is anti-cancerous, additionally deciphering neuroprotective activity in Parkinson's disease. This study demonstrates that C2 has a protective effect against rotenone induced cytotoxicity *in vitro* in human neuroblastoma SHSY5Y cells, through the reduction in levels of intracellular and mitochondrial ROS and through the suppression of caspase-3/caspase-9 activity. Based on these outcomes, it can be concluded that C2 might be a candidate for PD treatment.

We carried out an *in silico* analysis to elucidate the functional dynamics of the Cyclin B-cdc2 (CDK1) complex, which maintains a pivotal role in G2-M phase transition. Our investigation aimed to determine the potential of C2 as a CDK1 inhibitor, given its significant implications. The receptor molecule of CDK1 was evaluated using the ProtParam tool, as detailed in Table 2. Secondary structure prediction was conducted via the PROCHECK server, revealing 91.6% of residues in favoured regions, as depicted in Figure 4C. Non-bonded interactions were analysed using the ERRAT tool, yielding a quality factor of 95.15%, as shown in Figure 4B. The PROVE tool indicated that 2.6% of the protein atoms were buried outliers, illustrated in Figures 4A and 4D. All these analyses were performed using the SAVES server, with the VERIFY 3D tool confirming the overall affinity of atomic model (3D) along with its primary sequence. Figures 1D and 1E depict the docking complexes of C2 and Roscovitine for visualization. The binding free energy (ΔG) of C2 to CDK1 is -10.294742 kcal/mol, which is comparable to the known ΔG value of Roscovitine binding at -10.318 kcal/mol (Saraiva *et al.*, 2012). The hydrophobicity surface illustrates the hydrophobic nature of amino acids with colors ranging from the most hydrophilic residues (dodger blue) to 0.0 (white) and to the most hydrophobic residues (orange-red).

Surface binding analysis demonstrated that both Roscovitine and C2 occupy the same active site, forming a hydrophobic cleft on the surface of the CDK1 protein, as illustrated in the figure. The key residues within this binding pocket are detailed in Table 1. The interacting residues of C2 within the binding pocket were thoroughly analyzed, revealing interactions with specific residues, as depicted in Figure 1F. Considerably, Table 1 highlights the interacting residues within the binding pocket of C2, with GLU81 and LEU83 forming a molecular fork, a conserved feature across many CDKs, including CDK1. Notably, C2 interacts with LEU83, where the distance between the inhibitor and the NH group of LEU83 is 1.913 Å and C=O group is 2.673 Å. The docking study indicates that C2 binds to the active site (ATP binding pocket) of CDK1 with spontaneity comparable to other inhibitors, as evidenced by the ΔG values. Furthermore, C2 interacts with the molecular fork, similarly to other inhibitors. These findings strongly prove that C2 could potentially serve as an effective CDK1 inhibitor, akin to Roscovitine. Given that Roscovitine is recognized for its neuroprotective properties, our current study supports that C2 exhibits similar neuroprotective effects in context of neurodegenerative PD (Hilton *et al.*, 2008).

This study indicates that the 24 hr rotenone treatment caused the reduction in the viability of SH-SY5Y cells in a concentration-dependent mode and reflects a half-maximal inhibition (~54.41%) at 100 nM. Further, 4 hr prior treatment of C2 considerably improved the viability of the cells in a dose dependent manner producing an IC_{50} of C2 at 4 µM. From most of the reports, dysfunction of mitochondria and ROS are central to neurodegeneration in PD (Ashworth and Lord, 2018). Major sources of ROS generation are the mitochondrial respiratory chain (complexes I and III); complex I could lead to mitochondrial ROS production (Seaton *et al.*, 1997). Here we have observed high amount of ROS levels in rotenone induced model, which confirms oxidative stress, was indeed caused by rotenone treatment and this was reduced by C2 treatment.

Rotenone induces dopaminergic neuronal apoptosis via the MAPK and caspase-dependent signaling pathway Xicoy *et al.*, 2017. Cyt-c activates and enhances the release of the proenzyme caspase-9 (initiator) which activates the apoptotic effector caspase-3. Caspase-3 activation results in apoptosis through

activation of endonucleases that cleave endogenous substrates and cause death of neurons in Parkinson's. Caspases are initially synthesized as inactive precursors known as procaspases and activation through proteolytic cleavage lead to apoptosis. Also, the availability of the caspase precursors like pro caspase-2, 3, 8 and 9 was observed to be located in the intermembrane space of mitochondria based on the cell type. In the present study, the levels of caspases 8, 9 and 3 in the untreated SH-SY5Y cells were also observed to be upregulated as mentioned earlier. In SH-SY5Y cells with rotenone treatment, characteristics of apoptosis were observed i.e., there was an elevation in the levels of cytochrome c release, caspases- 3 and 9 and Bax while there was a decrease in Bcl-2. Therefore, due to the ability to protect mitochondria, C2 pretreatment reduced the expression of the apoptotic machinery and indicated that C2 possesses anti-apoptotic properties. In the present work, rotenone-treated apoptosis is associated with intracellular phosphorylation of p38/JNK MAPK proteins. Activation of p38/JNK MAPK proteins transforms induction of apoptosis via translocation of cytosolic Bax into mitochondria and the formation of permeable transition pore and the release of cytochrome c a death signal in the cytosol as shown by Western blotting. Treatment of C2 reduced the p38/JNK-activated apoptosis thereby protecting the neurons from undergoing apoptosis.

Despite the fact that for a long period of time PD was considered to be a nongenetic disorder of "sporadic" etiology, nowadays it is estimated that 5-10% of patients have monogenic subtypes of the disease that contributed to the development of drug targeted therapies. This is one of the first studies that show C2 can act as a potent CDK1 inhibitor which works as an anti-cancerous compound and deciphering its neuro-protective activities in Parkinson's disease. Therefore, in the developing the cause-directed therapies, further investigations of the effect of C2 on the expression of these genes may be explored in the treatment of PD.

AUTHOR CONTRIBUTIONS

Suresh Yerramsetty: Conceptualization, Methodology, Experimentation, Validation, Writing-original draft. Lavanya Ayyagari, Venkata Krishna Kanth Makani: Methodology, Validation, Data curation. Jolly Janette Mendonza, Suchitra Maheswari Ajjarapu: Docking Simulations and Analysis. Ahmed Kamal: Sourcing Compound. Manika Pal Bhadra, Smita C. Pawar: Supervision, Conceptualization, Investigation, Project administration, Funding acquisition.

ACKNOWLEDGEMENT

We acknowledge CSIR-IICT for evaluating the manuscript and providing with communication number IICT/Pubs/2022/106. We thank Late Mr. Akash Mallick, Periyasamy M, Ms. Paromita Das, Ms. Chitrakshi Pant, Ms. Kona Swathi for their support in providing experimental support.

CONFLICT OF INTEREST

The authors declare that there is no conflict of interest.

FUNDING

This work was supported by the Department of Biotechnology, New Delhi, India. Project Code: GAP770.

ABBREVIATIONS

PD: Parkinson's disease; **DA:** Dopamine; C2**:** (4-(2-(furan-2-ylmethylamino) benzoyl) piperazin-1-yl) (2-phenyl-7-(3:4:5-trimethoxyphenyl) pyrazolo[1:5-a]pyrimidin-5-yl) methanone; **ROS:** Reactive oxygen species; **SNPc:** substantia nigra pars compacta; **Cdk1:** Cyclin-dependent kinase 1; **AO:** Acridine orange; **EB:** Ethidium bromide; **ATP:** Adenosine triphosphate.

REFERENCES

Alharbi, B., Al-Kuraishy, H. M., Al-Gareeb, A. I., Elekhnawy, E., Alharbi, H., Alexiou, A., Papadakis, M., & Batiha, G. E.-S. (2024). Role of GABA pathway in motor and non-motor symptoms in Parkinson's disease: A bidirectional circuit. European Journal of Medical Research, 29(1), 205. https://doi.org/10.1186/s40001-024-01779-7 , PubMed: 38539252

Ashworth, A., & Lord, C. J. (2018). Synthetic lethal therapies for cancer: What's next after PARP inhibitors? Nature Reviews. Clinical Oncology, 15(9), 564–576. https://doi.org/10.1038/s41571-018-0055-6, PubMed: 29955114

Betarbet, R., Sherer, T. B., MacKenzie, G., Garcia-Osuna, M., Panov, A. V., & Greenamyre, J. T. (2000). Chronic systemic pesticide exposure reproduces features of Parkinson's disease. Nature Neuroscience, 3(12), 1301–1306. https://doi.org/10.1038/81834, PubMed: 11100151

Caboni, P., Sherer, T. B., Zhang, N., Taylor, G., Na, H. M., Greenamyre, J. T., & Casida, J. E. (2004). Rotenone, deguelin, their metabolites and the rat model of Parkinson's disease. Chemical Research in Toxicology, 17(11), 1540–1548. https://doi.org/10.1021/tx049867r, PubMed: 15540952

Chinta, S. J., & Andersen, J. K. (2005). Dopaminergic neurons. The International Journal of Biochemistry & Cell Biology, 37(5), 942–946. https://doi.org/10.1016/j.biocel.2004.09.009, PubMed: 15743669

Chipuk, J. E., & Green, D. R. (2008). How do BCL-2 proteins induce mitochondrial outer membrane permeabilization? Trends in Cell Biology, 18(4), 157–164. https://doi.org/10.1016/j.tcb.2008.01.007, PubMed: 18314333

Choong, C.-J., & Mochizuki, H. (2023). Involvement of mitochondria in Parkinson's disease. International Journal of Molecular Sciences, 24(23), Article 17027. https://doi.org/10.3390/ijms242317027, PubMed: 38069350

Cicenas, J., Kalyan, K., Sorokinas, A., Stankunas, E., Levy, J., Meskinyte, I., Stankevicius, V., Kaupinis, A., & Valius, M. (2015). Roscovitine in cancer and other diseases. Annals of Translational Medicine, 3(10), 135. https://doi.org/10.3978/j.issn.2305-5839.2015.03.61, PubMed: 26207228

Colovos, C., & Yeates, T. O. (1993). Verification of protein structures: Patterns of nonbonded atomic interactions. Protein Science, 2(9), 1511–1519. https://doi.org/10.1002/pro.5560020916, PubMed: 8401235

Guerrini, G., Ciciani, G., Costanzo, A., Daniele, S., Martini, C., Ghelardini, C., Di Cesare Mannelli, L., & Ciattini, S. (2013). Synthesis of novel cognition enhancers with pyrazolo[5,1-c][1,2,4]benzotriazine core acting at γ-aminobutyric acid type A (GABAA) receptor. Bioorganic and Medicinal Chemistry, 21(8), 2186–2198. https://doi.org/10.1016/j.bmc.2013.02.027, PubMed: 23490154

Hilton, G. D., Stoica, B. A., Byrnes, K. R., & Faden, A. I. (2008). Roscovitine reduces neuronal loss, glial activation and neurologic deficits after brain trauma. Journal of Cerebral Blood Flow and Metabolism, 28(11), 1845–1859. https://doi.org/10.1038/jcbfm.2008.75, PubMed: 18612315

Junn, E., & Mouradian, M. M. (2001). Apoptotic signaling in dopamine-induced cell death: The role of oxidative stress, p38 mitogen-activated protein kinase, cytochrome c and caspases. Journal of Neurochemistry, 78(2), 374–383. https://doi.org/10.1046/j.1471-4159.2001.00425.x, PubMed: 11461973

Kalyanaraman, B., Darley-Usmar, V., Davies, K. J. A., Dennery, P. A., Forman, H. J., Grisham, M. B., Mann, G. E., Moore, K., Roberts, L. J., & Ischiropoulos, H. (2012). Measuring reactive oxygen and nitrogen species with fluorescent probes: Challenges and

limitations. Free Radical Biology and Medicine, 52(1), 1–6. https://doi.org/10.1016/j.freeradbiomed.2011.09.030, PubMed: 22027063

Kamal, A., Tamboli, J. R., Ramaiah, M. J., Adil, S. F., Koteswara Rao, G., Viswanath, A., Mallareddy, A., Pushpavalli, S. N. C. V. L., & Pal-Bhadra, M. (2012). Anthranilamide-pyrazolo[1,5-a]pyrimidine conjugates as p53 activators in cervical cancer cells. ChemMedChem, 7(8), 1453–1464. https://doi.org/10.1002/cmdc.201200205

Kantari, C., & Walczak, H. (2011). Caspase-8 and bid: Caught in the act between death receptors and mitochondria. Biochimica et Biophysica Acta, 1813(4), 558–563. https://doi.org/10.1016/j.bbamcr.2011.01.026, PubMed: 21295084

Kasibhatla, S., Amarante-Mendes, G. P., Finucane, D., Brunner, T., Bossy-Wetzel, E., & Green, D. R. (2006). Acridine orange/ethidium bromide (AO/EB) staining to detect apoptosis. CSH Protocols, 2006(3), Article pdb.prot4493. https://doi.org/10.1101/pdb.prot4493, PubMed: 22485874

Kona, S. V., & Kalivendi, S. V. (2024). The USP10/13 inhibitor, spautin-1, attenuates the progression of glioblastoma by independently regulating RAF-ERK mediated glycolysis and SKP2. Biochimica et Biophysica Acta. Molecular Basis of Disease, 1870(7), Article 167291. https://doi.org/10.1016/j.bbadis.2024.167291, PubMed: 38857836

Li, J., Spletter, M. L., Johnson, D. A., Wright, L. S., Svendsen, C. N., & Johnson, J. A. (2005). Rotenone-induced caspase 9/3-independent and -dependent cell death in undifferentiated and differentiated human neural stem cells. Journal of Neurochemistry, 92(3), 462–476. https://doi.org/10.1111/j.1471-4159.2004.02872.x, PubMed: 15659217

McClue, S. J., Blake, D., Clarke, R., Cowan, A., Cummings, L., Fischer, P. M., MacKenzie, M., Melville, J., Stewart, K., Wang, S., Zhelev, N., Zheleva, D., & Lane, D. P. (2002). In vitro and in vivo antitumor properties of the cyclin dependent kinase inhibitor CYC202 (R-roscovitine). International Journal of Cancer, 102(5), 463–468. https://doi.org/10.1002/ijc.10738, PubMed: 12432547

Pettersen, E. F., Goddard, T. D., Huang, C. C., Couch, G. S., Greenblatt, D. M., Meng, E. C., & Ferrin, T. E. (2004). UCSF Chimera—A visualization system for exploratory research and analysis. Journal of Computational Chemistry, 25(13), 1605–1612. https://doi.org/10.1002/jcc.20084, PubMed: 15264254

Qin, H., Srinivasula, S. M., Wu, G., Fernandes-Alnemri, T., Alnemri, E. S., & Shi, Y. (1999). Structural basis of procaspase-9 recruitment by the apoptotic protease-activating factor 1. Nature, 399(6736), 549–557. https://doi.org/10.1038/21124, PubMed: 10376594

Ramaiah, M. J., Pushpavalli, S. N. C. V. L., Lavanya, A., Bhadra, K., Haritha, V., Patel, N., Tamboli, J. R., Kamal, A., Bhadra, U., & Pal-Bhadra, M. (2013). Novel anthranilamide-pyrazolo[1,5-a]pyrimidine conjugates modulate the expression of p53-MYCN associated micro RNAs in neuroblastoma cells and cause cell cycle arrest and apoptosis. Bioorganic and Medicinal Chemistry Letters, 23(20), 5699–5706. https://doi.org/10.1016/j.bmcl.2013.08.018, PubMed: 23992861

Ramu, G., Tangella, Y., Ambala, S., & Nagendra Babu, B. N. (2020). Regioselective ring expansion of 3-Ylideneoxindoles with Tosyldiazomethane (TsDAM): A metal-free and greener approach for the synthesis of pyrazolo-[1,5-c]quinazolines. The Journal of Organic Chemistry, 85(8), 5370–5378. https://doi.org/10.1021/acs.joc.0c00078, PubMed: 32227895

Reeve, A., Simcox, E., & Turnbull, D. (2014). Ageing and Parkinson's disease: Why is advancing age the biggest risk factor? Ageing Research Reviews, 14(100), 19–30. https://doi.org/10.1016/j.arr.2014.01.004, PubMed: 24503004

Sahoo, S., Kumari, S., Pulipaka, S., Chandra, Y., & Kotamraju, S. (2024). SIRT1 promotes doxorubicin-induced breast cancer drug resistance and tumor angiogenesis via regulating GSH-mediated redox homeostasis. Molecular Carcinogenesis, 63(12), 2291–2304. https://doi.org/10.1002/mc.23809, PubMed: 39136605

Saraiva, L. A., Veloso, M. P., Camps, I., & da Silveira, N. J. F. (2011). Structural bioinformatics approach of cyclin-dependent kinases 1 and 3 complexed with inhibitors. Molecular Informatics, 30 (2–3), 219–231. https://doi.org/10.1002/minf.201000143, PubMed: 27466775

Saraiva, R. A., Bueno, D. C., Nogara, P. A., & Rocha, J. B. (2012). Molecular docking studies of disubstituted diaryl diselenides as mammalian δ-aminolevulinic acid dehydratase enzyme inhibitors. Journal of Toxicology and Environmental Health. Part A, 75 (16–17), 1012–1022. https://doi.org/10.1080/15287394.2012.697810, PubMed: 22852851

Seaton, T. A., Cooper, J. M., & Schapira, A. H. (1997). Free radical scavengers protect dopaminergic cell lines from apoptosis induced by complex I inhibitors. Brain Research, 777 (1–2), 110–118. https://doi.org/10.1016/s0006-8993(97)01034-2, PubMed: 9449419

Slee, E. A., Harte, M. T., Kluck, R. M., Wolf, B. B., Casiano, C. A., Newmeyer, D. D. et al. (1999). Green and S.J. Martin. Ordering Cytochrome C-Initiated Caspase Cascade Hierarchical Activation Caspases, 144(2);2(3), -6, -7, -8 and -10 in a caspase-9-dependent manner," The Journal of cell biology, 281–292.

Smith, P. D., Crocker, S. J., Jackson-Lewis, V., Jordan-Sciutto, K. L., Hayley, S., Mount, M. P., O'Hare, M. J., Callaghan, S., Slack, R. S., Przedborski, S., Anisman, H., & Park, D. S. (2003). Cyclin-dependent kinase 5 is a mediator of dopaminergic neuron loss in a mouse model of Parkinson's disease. Proceedings of the National Academy of Sciences of the United States of America, 100(23), 13650–13655. https://doi.org/10.1073/pnas.2232515100, PubMed: 14595022

Srivastava, P., & Panda, D. (2007). Rotenone inhibits mammalian cell proliferation by inhibiting microtubule assembly through tubulin binding. The FEBS Journal, 274(18), 4788–4801. https://doi.org/10.1111/j.1742-4658.2007.06004.x, PubMed: 17697112

Van Den Eeden, S. K., Tanner, C. M., Bernstein, A. L., Fross, R. D., Leimpeter, A., Bloch, D. A., & Nelson, L. M. (2003). Incidence of Parkinson's disease: Variation by age, gender and race/ethnicity. American Journal of Epidemiology, 157(11), 1015–1022. https://doi.org/10.1093/aje/kwg068, PubMed: 12777365

Xicoy, H., Wieringa, B., & Martens, G. J. M. (2017). The SH-SY5Y cell line in Parkinson's disease research: A systematic review. Molecular Neurodegeneration, 12(1), 10. https://doi.org/10.1186/s13024-017-0149-0, PubMed: 28118852.

Cite this article: Yerramsetty S, Ayyagari L, Makani VKK, Mendonza JJ, Ajjarapu SM, Kamal A, *et al*. Neuroprotective and Anti-Apoptotic Activity of Anthranilamide Pyrazolo[1,5-a] Pyrimidine Derivative against Parkinson's Disease Model in Rotenone-Induced SH-SY5Y Cells. Int. J. Pharm. Investigation. 2025;15(2):471-81.